Available online at www.sciencedirect.com
SCIENCE DIRECT®
Journal of Sound and Vibration 277 (2004) 327–351
JOURNAL OF SOUND AND VIBRATION
www.elsevier.com/locate/jsvi

Experimental study of non-linear effects in a typical shear lap joint configuration

C.J. Hartwigsen[a], Y. Song[b], D.M. McFarland[b,*], L.A. Bergman[b], A.F. Vakakis[c,d]

[a] *Sandia National Laboratories, Albuquerque, NM 87185, USA*
[b] *Department of Aeronautical and Astronautical Engineering, University of Illinois at Urbana-Champaign, 306 Talbot Laboratory, MC-236, Urbana, IL 61801-2935, USA*
[c] *Division of Mechanics, National Technical University of Athens, P.O. Box 64042, GR-157 10 Zografos, Greece*
[d] *Department of Mechanical and Industrial Engineering, University of Illinois at Urbana-Champaign, Urbana, IL 61801, USA*

Received 25 February 2003; accepted 1 September 2003

Abstract

Although mechanical joints are integral parts of most practical structures, their modelling and their effects on structural dynamics are not yet fully understood. This represents a serious impediment to accurate modelling of the dynamics and to the development of reduced-order, finite element models capable of describing the effects of mechanical joints on the dynamics. In this work we provide an experimental study to quantify the non-linear effects of a typical shear lap joint on the dynamics of two structures: a beam with a bolted joint in its center; and a frame with a bolted joint in one of its members. Both structures are subjected to a variety of dynamical tests to determine the non-linear effects of the joints. The tests reveal several important influences on the effective stiffness and damping of the lap joints. The possibility of using Iwan models to represent the experimentally observed joint effects is discussed.

1. Introduction

The purpose of this work is to experimentally study the effects of a shear lap joint on the dynamic response of a structure. The actual physics taking place at the lap joint interface of a vibrating structure is complex and not fully understood. The reason is that there exist many parameters and uncertainties that prevent an accurate understanding and modelling of the joint

*Corresponding author. Tel.: +1-217-244-9573; fax: +1-217-244-0720.
E-mail addresses: cjhartw@sandia.gov (C.J. Hartwigsen), dmmcf@uiuc.edu (D.M. McFarland), lbergman@uiuc.edu (L.A. Bergman), vakakis@central.ntua.gr, avakakis@uiuc.edu (A.F. Vakakis).

0022-460X/$ - see front matter
doi:10.1016/j.jsv.2003.09.018

physics; these include interface area, distribution of normal and shear forces at the interface, surface finish, and history-dependent and non-linear effects in the dynamics.

Lap joints seem to exhibit two types of motion during vibration: *microslip/slap* and *macroslip/slap* [1]. As force is applied to a joint, small regions of the interface area will break free and begin slipping; these localized motions are termed *microslip*. It is important to note that the actual parts composing the joint do not move in relation to each other on a macrolevel during microslip or microslap, but the motions occur only over small regions of the interface area. As the level of the force applied to the joint increases, a larger portion of the interface will break free and slip; eventually, the entire contact area will be slipping, which is termed *macroslip*. For most joints excited at reasonable force levels, macroslip does not occur, but microslip is common. The small, localized motions during microslip result in energy losses at the joint, which is perceived as localized damping of the structure. Indeed, most damping effects encountered in practical structures are taking place at jointed interfaces [2].

Beards [3] performed a series of experiments that showed that damping in joints is much larger than material damping; his work focused on using joint damping for vibration control. Gaul and Lenz [4] performed experiments and analyses on a bolted single-lap joint located between two large masses and excited with axial and torsional sinusoidal forces. Their studies revealed that hysteresis loops measured for different excitation force levels had different slopes—as the force was increased, the slope decreased, indicating a softening system. The experiments showed two general slopes for the force-deflection curves, and two distinct regions in the dissipated energy per cycle vs. displacement; these were attributed to microslip and macroslip. Goodman [5] analytically studied interfaces that experienced localized slipping. He found that for a wide variety of joints, a power law could be established between the force input to a system and the energy dissipated per cycle of loading. When the interface was described using Coulomb friction, the exponent of the power law was equal to 3, which is identical to that corresponding to the contact of two elastic spheres under cyclic tangential loads [6].

Further investigations into axial joints have been undertaken at Sandia National Laboratories [7,8], aimed at identifying the physics at the joint interface. A series of closely controlled experiments was able to establish that there exists a power-law relationship between input force and energy dissipated per cycle [9], and further experimental results identified the regions of microslip. A highly detailed finite element (FE) model for a single shear lap joint containing hundreds of thousands of degrees of freedom (d.o.f.) was constructed at Sandia that seems to predict joint physics with some degree of precision [10]. The model confirmed the aforementioned power-law relation, although the predicted slope was different from the measured one. Such a model, however, would be impractical for representing the dynamics of real structures containing many joints. Further work at Sandia examined the use of Iwan models [11] to describe the dynamics of joints [12,13]. The Iwan model consists of a continuum network of springs and sliders, with the break-free forces of the sliders being described by a distribution function. Different distribution functions lead to different power laws in the diagrams of input force vs. energy dissipated per cycle.

There are several different approaches that can be followed toward investigating joint dynamics. One is to try to identify the actual physics taking place within the joint on a microscale; some of the experiments mentioned above follow this approach. An alternative direction is to look at the effect of the joint on the overall dynamics of the structure. In this approach, the

microphysics need not necessarily be considered (or modelled) in detail, but rather the overall dynamical effect of the full joint needs to be examined. This work follows the second approach. The ultimate goal of the authors' research on mechanical joints is the development of a reduced-order model capable of accurately incorporating the effects of the joint into a structural model. Towards this aim, an experimental study is performed to identify the principal joint effects on the structural dynamics. Qualitative trends in the measurements are identified, and the suitability of capturing these effects with Iwan models is addressed.

2. Structure I: beam with shear lap joint

Since the research effort described in this work focuses on examining the effects of a joint on the overall structural dynamics of a bolted system, one initially wishes to consider a test piece with simple configuration in order to understand the basic qualitative features of the effects of a local bolted joint on the dynamics. Moreover, for comparison purposes, in addition to building a structure with a bolted joint interface (the *jointed structure*), we also build a structure possessing identical geometrical and material properties to the jointed structure, but with no joint interface (the *monolithic structure*). The premise is that under identical forcing and boundary conditions, subtraction of the dynamics of the jointed and monolithic structures will provide the effect of the joint on the dynamics. A similar approach was adopted in an earlier experimental work [14] where laser vibrometry was used to quantify the difference in the dynamics between two jointed and monolithic beams, and an ad hoc model was introduced to interpolate this difference.

The first structure considered is depicted in Fig. 1(a). It was designed in conjunction with Sandia National Laboratories and consists of a 20.25 in × 1 in × 0.25 in simple beam made of low-carbon steel with (jointed beam) or without (monolithic beam) a shear lap joint in its center. Details of the dimensions of the components of the lap joint can be found in Ref. [15]. A first series of modal analysis experiments was performed to detect the effects of the joint on the structural dynamics. Free boundary conditions were simulated in the tests by suspending the beams at their two ends from the ceiling with a 6 ft long length of nylon cord. Extensive repeatability tests were performed prior to each experiment to assure reproducibility of the

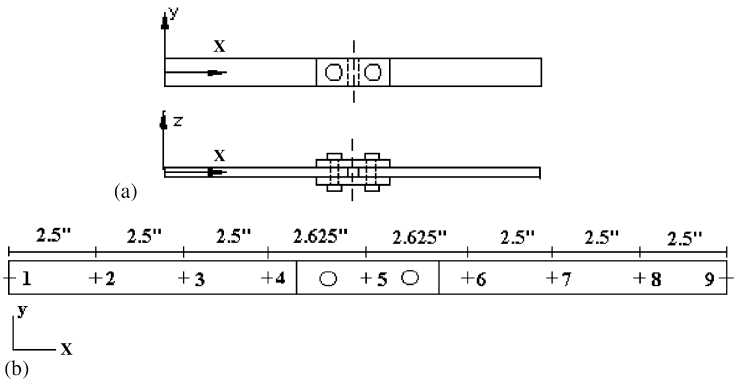

Fig. 1. Structure I: (a) configuration and (b) sensing locations.

boundary conditions. The input forces were applied with a modal hammer (impulsive excitations), and nine sensing positions on each beam were considered; these are depicted in Fig. 1(b). The hammer tests were conducted as roving-input tests, meaning that the accelerometer stayed fixed at sensing location 4 for every test, while the hammer excitation was applied at all nine measurement points in succession. Input forces and output accelerations were considered only in the z direction, that is, perpendicular to the beams. All measured data was transferred to PC-based Matlab for post-processing and analysis. Diamond modal analysis software, written at Los Alamos National Laboratory, was used within Matlab to perform the modal analysis; the rational polynomial method was used to fit the peaks of the frequency response functions (FRFs) to determine the modal parameters.

In Fig. 2 we depict the inertance FRFs (acceleration over force) of the monolithic beam with bolts and of the jointed beam. The FRFs are driving-point functions, measured at location 4 (cf. Fig. 1(b)). We note the qualitative difference between the two FRFs: Not only have the upper peaks shifted in frequency, but, in addition, some peaks have changed in shape, indicating a damping change. The third peak, close to 760 Hz, is of particular interest, because for the monolithic beam this peak is quite prominent, while for the jointed beam it is nearly eliminated. (It turns out that this is due to the slight distortion of the modes due to the joint: location 4 is close to a node of the third mode of the jointed beam.) Such differences in the dynamics highlight the necessity of taking joints into account when modelling practical structures. Table 1 shows the natural frequencies and modal damping ratios resulting from the modal analysis. The damping ratios were measured assuming viscous damping, and using the 'peak amplitude' method [15]. As expected, the jointed beam exhibits much larger damping factors for all modes. In addition, all modes of the jointed beam have shifted down in frequency, with a larger shift seen in the higher

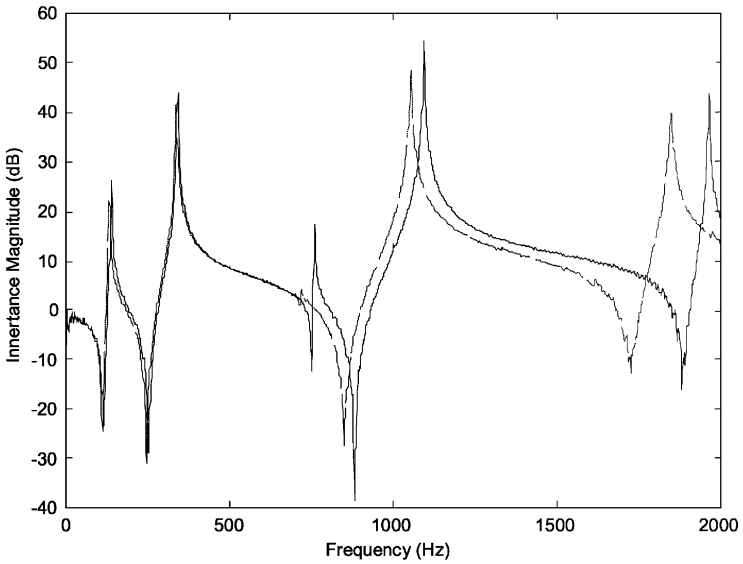

Fig. 2. Comparison of driving point inertance FRFs for the monolithic beam with bolts (dark, solid curve) and the jointed beam (light, broken curve).

Table 1
Modal parameters of the monolithic and jointed beams

Natural frequencies (Hz)			Modal damping ratios (%)		
No.	Monolithic beam with bolts	Jointed beam	No.	Monolithic beam with bolts	Jointed beam
f_1	139.04	132.26	ζ_1	0.12	0.69
f_2	341.32	336.80	ζ_2	0.05	0.15
f_3	757.99	715.43	ζ_3	0.04	0.13
f_4	1092.64	1052.37	ζ_4	0.03	0.11
f_5	1962.57	1846.62	ζ_5	0.02	0.18

frequencies; the 5th mode shifts by almost 130 Hz, a change of 6.6%. The observed modes are the expected first 5 flexural mode shapes for a beam.

Clearly, the assumption of viscous damping seems to be an oversimplification, given that non-linear dissipation mechanisms are expected to exist at the joint interface. In order to study more accurately the damping effects, and to check the small damping values identified by the peak amplitude method an alternative approach was adopted. Since this method will be used repeatedly in this work we describe it briefly. This non-parametric method (it does not assume a priori a specific type of damping) can be considered as an extension of the envelope decay method used for time-domain damping identification for single-d.o.f. systems, and can lead to more accurate results for lightly damped or non-viscously damped structures. The method relies on observing the decay envelope for time responses to impact excitations, since the nature of this decay provides reliable insight into the modal damping mechanism [16].

For the second series of tests of Structure I the accelerometer was set either at sensing position 4 or at the center of the system, for measuring even- or odd-numbered modes, respectively. Again, an impact hammer was used to impulsively excite the structure. Three different forcing levels of increasing strength were used. Although it is not possible to precisely control the magnitude of the impact from a hand-held hammer, the idea was to excite the structure at a very low level and at progressively higher levels to observe any differences in response due to joint non-linearities. The results from the second series of experiments show that the structure has some interesting dynamic properties. In Figs. 3(a) and (b) we depict the high frequency (0–2000 Hz) time responses to soft and hard hammer hits for the jointed beam. As can be seen in the results, the soft hammer hit caused a response that appears to be decaying exponentially; the hard hit, however, caused a response that initially decays very rapidly, but then reverts to a nearly exponential decay once the level of vibration decreases sufficiently. The qualitative change in the behavior of the envelope with increasing force is attributed to non-linear damping effects at the joint interface.

The envelope of the transient decay can be established by taking the Hilbert transform of the time response, $H = \text{Hilbert}(x)$, and then computing the envelope as $E = \sqrt{H^2 + x^2}$. In order to study the modal damping of a specific mode, the structural response was filtered close to that mode's frequency using a 10th order Butterworth filter in Matlab. Using the filtered data the envelope decay computations for each of the modes could be carried out, and post-processing for studying the modal damping factors could be performed.

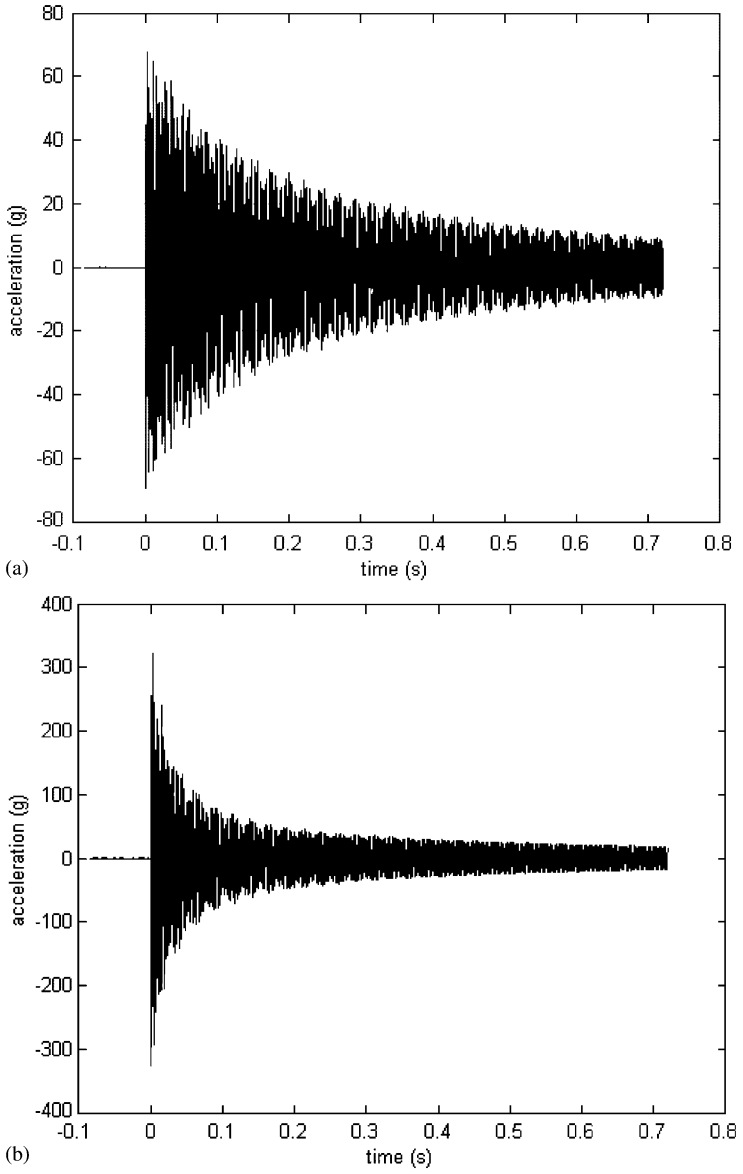

Fig. 3. Time response, 0–2000 Hz bandwidth, of the jointed beam following (a) soft and (b) hard hammer hits.

In the case of the monolithic beam, the free decay for each mode was nearly exponential. In Fig. 4 we depict the time response and the logarithm of the envelope for the 1st mode close to 140 Hz. The logarithm of the envelope plots as a straight line, indicating nearly linear viscous damping for that mode; the slope of the logarithm of the envelope yields the modal damping ratio. The envelope decays for the leading five modes of the monolithic beam indicate linear viscous modal damping, and their corresponding values are presented in Table 2 along with their

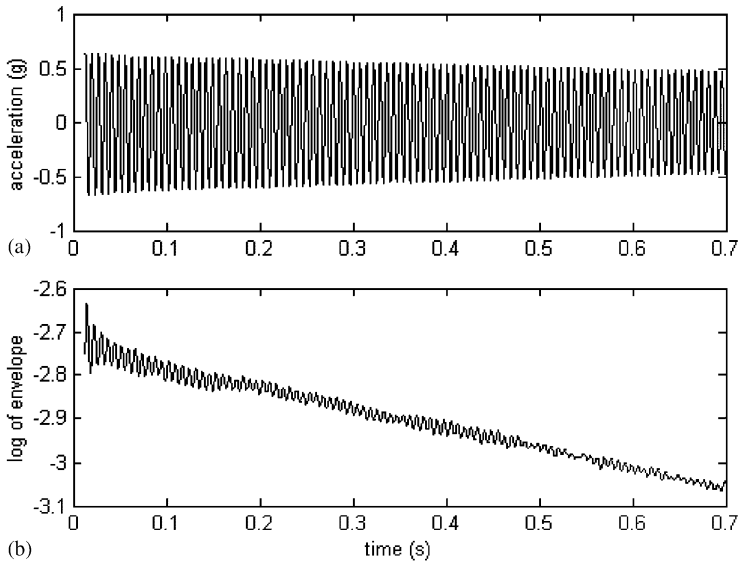

Fig. 4. Filtered transient response and logarithm of the envelope for the first mode (139 Hz) of the monolithic beam: (a) acceleration time response and (b) logarithm of the response envelope.

Table 2
Experimentally determined damping factors for the monolithic beam

No.	Natural frequency (Hz)	Damping factors frequency domain analysis (%)	Damping factors time domain analysis (%)
f_1	139.04	0.12	0.09
f_2	341.32	0.05	0.02
f_3	757.99	0.04	0.02
f_4	1092.64	0.03	0.02
f_5	1962.57	0.02	0.01

comparisons with the corresponding estimates from the frequency-domain modal analysis. Although smaller, the time-domain estimates are comparable to the ones derived by frequency-domain analysis.

Computing modal damping estimates for the jointed beam was not so straightforward. In Fig. 5 the transient response to a hard hit of the filtered first mode of the system is depicted. The upper plot in this figure shows that the mode initially decays very rapidly, but then settles to a more gradual decay as the amplitude decreases. The lower plot shows the logarithm of the envelope, which after an initial stage ($t<0.4$ s) reaches a straight-line asymptote. This implies that at high amplitudes the damping at the joint is non-viscous; however, once the amplitude diminishes the non-linear effects are eliminated and the system approaches a viscous damping limit. As the envelope of the jointed system decay is not purely exponential, it cannot be described with a single numerical damping factor. However, the envelope can be divided into intervals, each of which can be approximated with an equivalent viscous damping factor. Fig. 6 depicts the equivalent

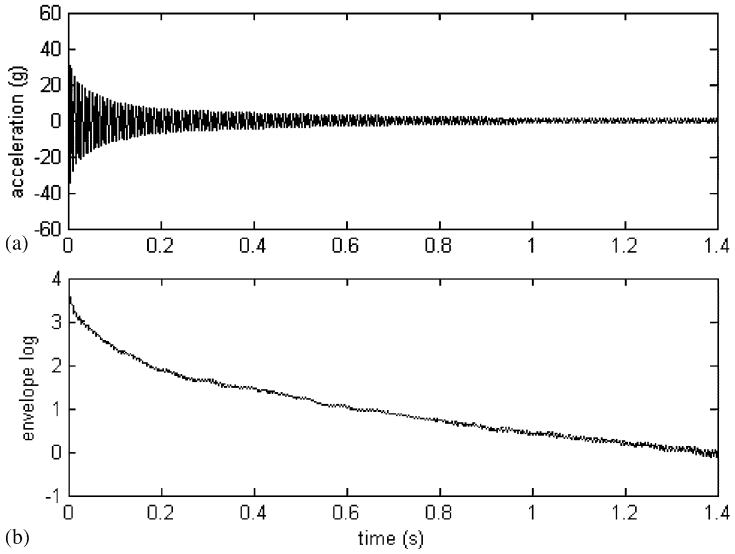

Fig. 5. Filtered transient response and logarithm of the envelope for the first mode (132 Hz) of the jointed beam: (a) acceleration time response and (b) logarithm of the response envelope.

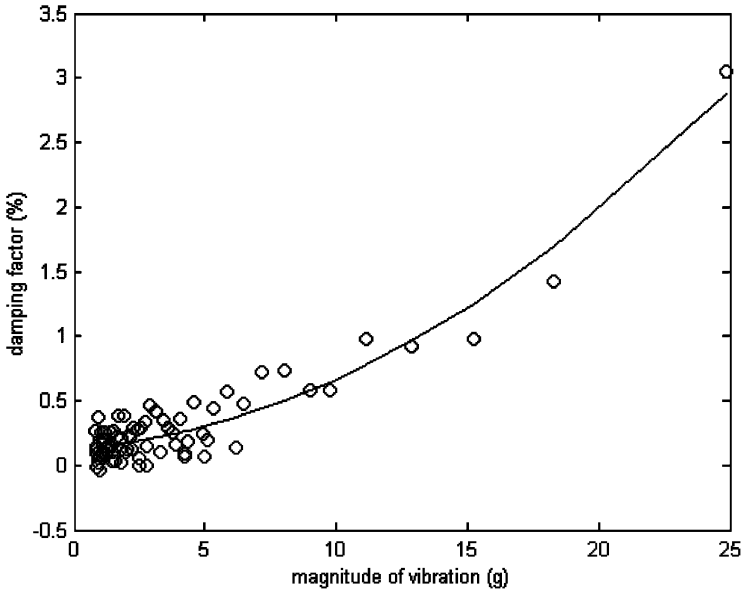

Fig. 6. Equivalent viscous damping ratio vs. vibration magnitude for the first mode of the jointed beam (132 Hz): symbols, experimental data; solid curve, fitted function.

damping factor plotted against the amplitude of vibration for each interval when the envelope is divided into 50 equal intervals. The spread of the data can be attributed to the non-smooth envelope decay of the filtered transient response as evidenced by the plots of Fig. 5. (Physically

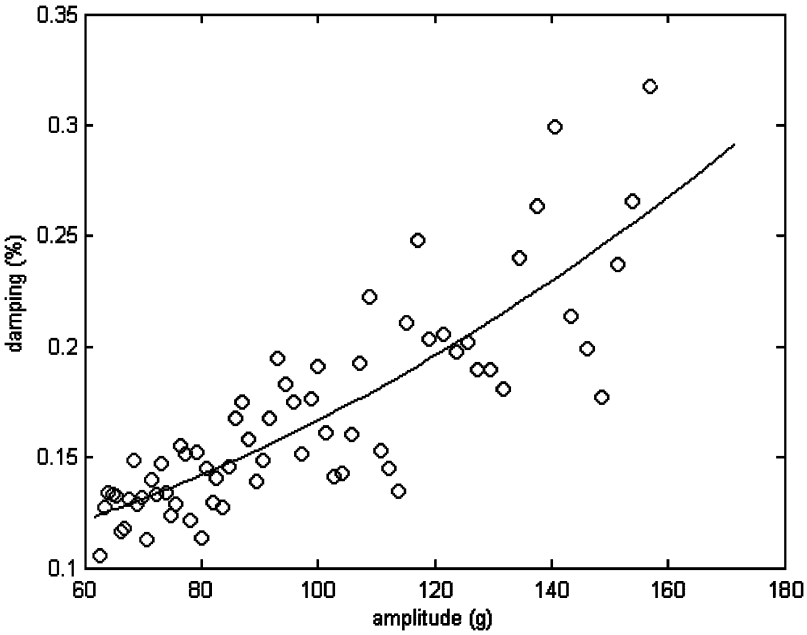

Fig. 7. Equivalent viscous damping ratio vs. vibration magnitude for the second mode of the jointed beam (337 Hz): symbols, experimental data; solid curve, fitted function.

unrealistic negative damping values have been retained in this and subsequent plots in the belief that they distort the statistical results less than would eliminating these points.) However, the data seem to follow the best-fit polynomial of degree 2 fairly well. When the vibration amplitude is high (around 25 g), the equivalent damping factor is also relatively high (near 3%); as the amplitude subsides the equivalent damping ratio also drops (to less than 0.5%). Similar equivalent viscous damping ratios were computed for the next four modes of the jointed beam, and are depicted in Figs. 7–10. These results show trends similar to those observed for the first mode: At high vibration levels the structure shows high levels of damping ($\sim$3–4%), which causes the vibration to subside rapidly, and, in turn, the damping approaches smaller, linear viscous behavior. The second and fourth modes do not exhibit this non-linear damping phenomenon strongly. A clear explanation for this is that the center of the beam (where the joint is located) represents a node for these modes, preventing much curvature of the joint; this reduces the joint effect while the structure is vibrating in these two modes. By contrast, for the odd-numbered modes the joint lies at a point of high curvature, which amplifies the non-linear joint effects on the dynamics.

A third aspect of the experimental study of Structure I concerns the energy dissipated per cycle during steady state vibration. It has been established from the previous results that damping is higher for the jointed structure than the monolithic one, and that damping is amplitude-dependent. The question remains of how energy is dissipated within the structure. An analysis by Goodman [5] showed that for a system with linear viscous damping, energy is dissipated in a power 2 relationship with respect to input force. For a system with sliding friction, the dissipated energy obeys a power 3 law. The power laws relating energy dissipation to input force for the

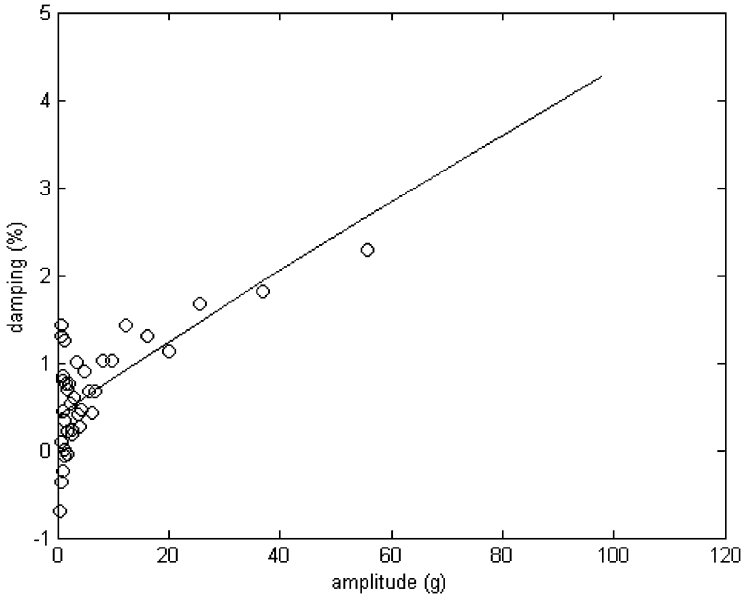

Fig. 8. Equivalent viscous damping ratio vs. vibration magnitude for the third mode of the jointed beam (715 Hz): symbols, experimental data; solid curve, fitted function.

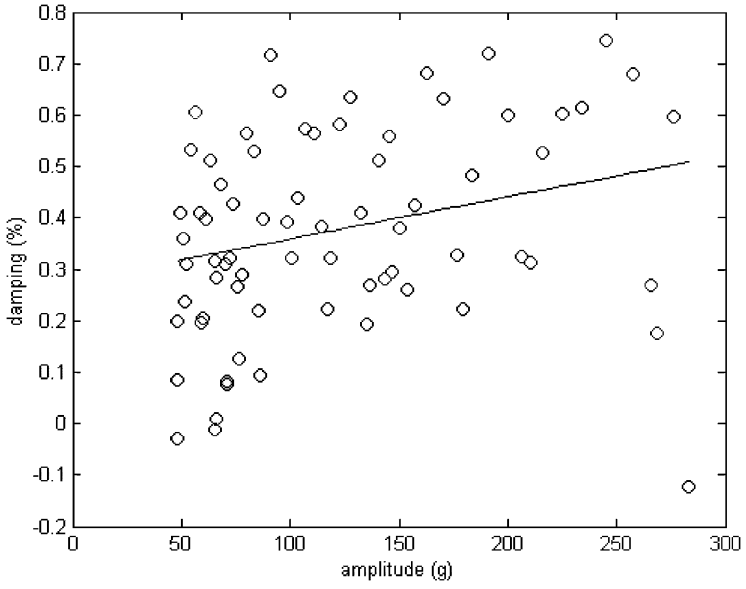

Fig. 9. Equivalent viscous damping ratio vs. vibration magnitude for the fourth mode of the jointed beam (1052 Hz): symbols, experimental data; solid curve, fitted function.

monolithic and jointed beams were studied to determine if they complied with the corresponding theoretical estimates. For this third series of experiments harmonic input force was provided by means of an electromagnetic shaker connected to the structure through a stinger. The force was

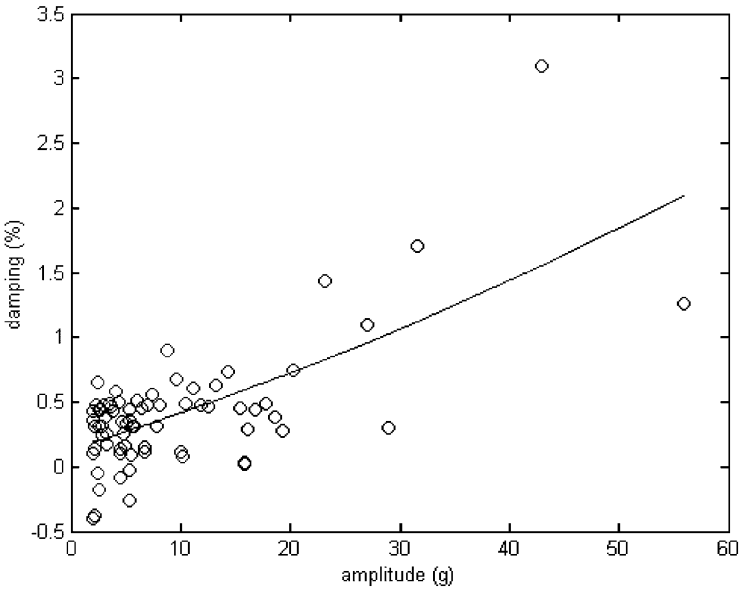

Fig. 10. Equivalent viscous damping ratio vs. vibration magnitude for the fifth mode of the jointed beam (1847 Hz): symbols, experimental data; solid curve, fitted function.

applied normal to the beam at sensing location 5 (its middle), with the accelerometer attached at the same location. The frequency of the input force was restricted to the neighborhood of the first mode. The experimental procedures are described in detail elsewhere [15] and will not be included here.

The energy dissipated per cycle was assessed following Smallwood et al. [8], by directly measuring the magnitude of the transmissibility ratio at resonance, Q. Assuming that this quantity has the amplitude dependence $Q = KA^{-n}$ (where A is the steady state amplitude of the acceleration and parameters K and n are measurable from experimental data), it can be shown [15] that for a non-linearly damped mode the energy dissipated per cycle, E, is computed from the expression

$$\log(E) = \log\left(\frac{\pi m}{K\omega^4}\right) + (2+n)\log(A), \tag{1}$$

where m is a parameter. This means that E exhibits a power-law relationship with respect to the amplitude of vibration, as expected. The number n represents the portion of the power-law exponent that corresponds to non-linear damping, and can be independently estimated by considering the relationship between Q and A, which can be directly measured from resonance tests. The above process is defined at resonance, which means resonance must be tracked. The only effect of varying the driving frequency is to change the term $\log[\pi m/(K\omega^4)]$, which varies by only 0.2% when tracking the resonance of the jointed beam (practically, it can be assumed constant). Figs. 11 and 12 depict the log–log plots of Q vs. the amplitude of acceleration for the jointed and monolithic systems, respectively. The slope of the plot for the monolithic system

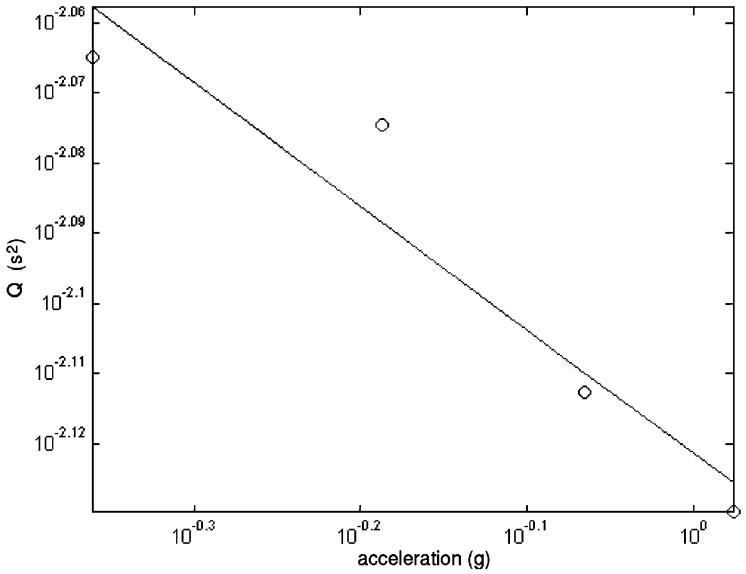

Fig. 11. Log–log plot of Q vs. amplitude of acceleration for the monolithic beam: symbols, experimental data; solid curve, fitted function.

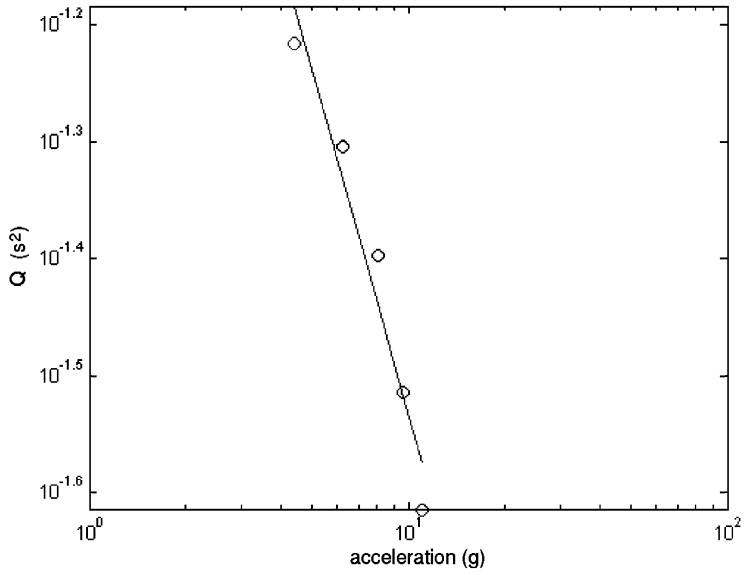

Fig. 12. Log–log plot of Q vs. amplitude of acceleration for the jointed beam: symbols, experimental data; solid curve, fitted function.

is $-n = -0.17$, which gives a value of 2.17 for the exponent of the power-law relation between amplitude of vibration and energy dissipated. This is close to the theoretical linear value of 2. Considering the plot of Fig. 12, corresponding to the jointed system, the identified value is

$-n = -0.98$, which gives an exponent of 2.98 for the power-law between energy dissipated per cycle and input force. This is close to the theoretical value of 3 corresponding to sliding friction.

The analysis of the dynamics of Structure I provided some insight into the non-linear joint damping effects on the structural dynamics. In the next section we will apply some of the methodologies discussed above to a jointed frame, a more practical geometric configuration, labeled Structure II, in order to identify and quantify the effects of its joints on the dynamics.

3. Structure II: frame with shear lap joint

Structure II is a rectangular frame also designed at Sandia National Laboratories, and is depicted in Fig. 13. In the center of one of its longitudinal beams there is a lumped mass consisting of two plates welded onto the frame leg, whereas in the center of its other longitudinal beam there is a shear lap joint of the same design as that in Structure I. Two lap plates are used, one on either side, with a single bolt on each side of the joint. As with Structure I, two experimental rigs were constructed: one, the *jointed frame*, consisted of the frame with a cut in one of its longitudinal beams, two lap plates, and bolts; this frame had to be joined together at the cut. The second rig, the *monolithic frame*, was manufactured to the same dimensions, but in place of the bolted joint

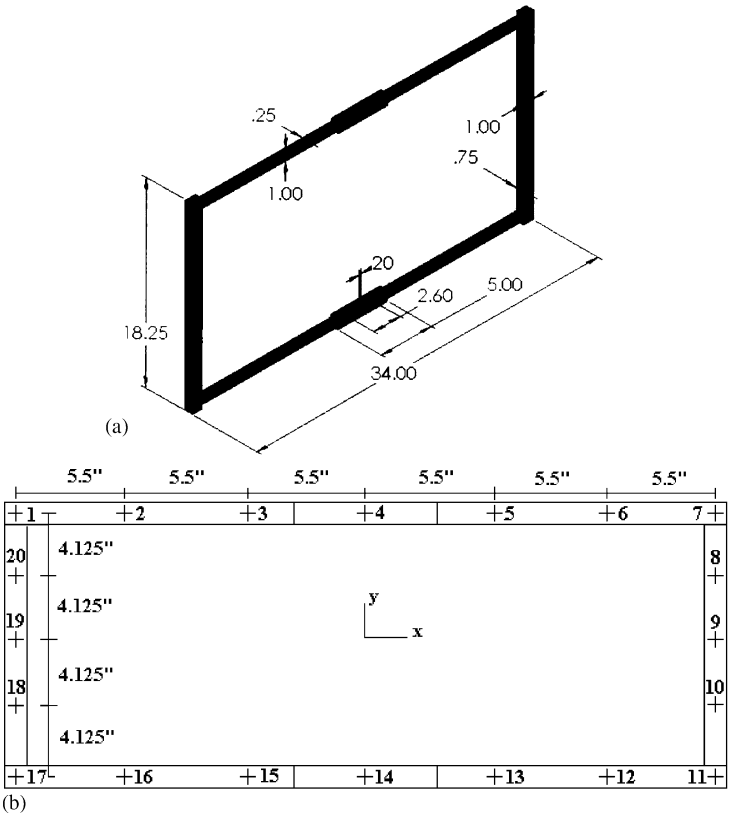

Fig. 13. Structure II: (a) configuration and (b) sensing locations.

the plates were welded onto the cut leg of the frame; this was meant to simulate a monolithic (homogeneous) structure. It should be noted that the corners of both frames were also welded together. Throughout the experiments, it was assumed that the welded joints behaved as if the structure was monolithic at the welds. While a welded joint does exhibit to a certain extent interfacial non-linear effects, it is a much stiffer joint with less motion at the interfaces than would occur in a bolted joint of similar size. Indeed, as discussed below the low damping factors extracted for the monolithic structure indicate that there was little frictional energy loss at the welded joints.

First a series of hammer tests was performed to identify the natural frequencies and modal damping ratios of the jointed and monolithic frames with free boundary conditions. To this end, the structure was suspended using two 6 ft lengths of nylon cord, in an effort to simulate free boundary conditions. Data were taken at 20 different positions on each frame, as shown in Fig. 13(b). Input forces and output accelerations were always applied and measured in the $z$direction, i.e., perpendicular to the frames. The impulsive hammer excitation was applied at three different locations on the frame, namely at locations 2, 3 and 4; this was necessary because the frame had several pairs of double modes (modes that occurred at close frequencies).

Modal analysis reveals that the monolithic frame possesses a total of 10 modes with out-of-plane motion between 0 and 500 Hz; in addition, there is an in-plane mode at 85 Hz. Among these, there are three pairs of closely spaced modes, near 25, 85 and 315 Hz. Fig. 14 depicts the comparison of the driving-point FRFs for the jointed and monolithic frames with force applied and acceleration measured at sensing location 3 (cf. Fig. 13(b)). This comparison reveals similar trends to those observed for Structure I. Generally, the natural frequencies shift down and the modal damping ratios increase when the joint is added. Table 3 lists the natural frequencies and

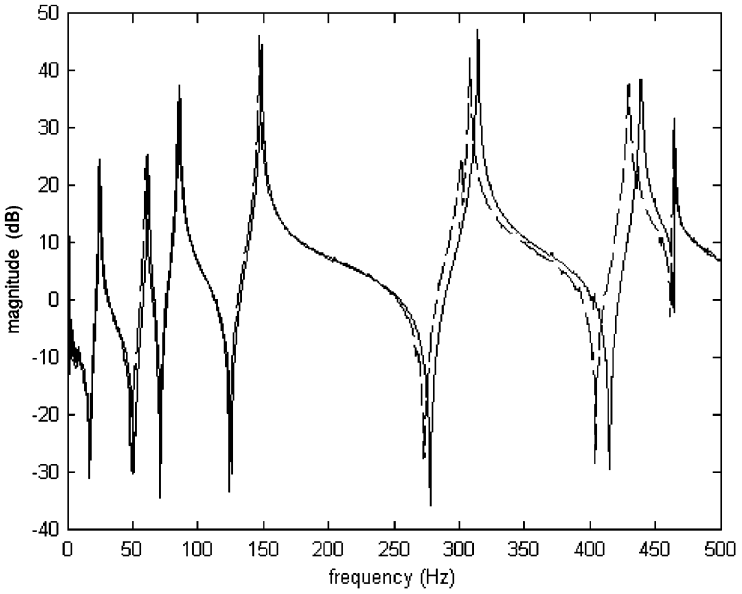

Fig. 14. Comparison of driving point inertance FRFs for the monolithic (dark, solid curve) and jointed (light, broken curve) frames.

Table 3
Modal parameters of the monolithic and jointed frames

Natural frequencies (Hz)			Modal damping ratios (%)		
No.	Monolithic frame	Jointed frame	No.	Monolithic frame	Jointed frame
f_1	24.62	24.29	ζ_1	0.04	0.12
f_2	25.30	24.41	ζ_2	0.06	0.26
f_3	61.99	60.14	ζ_3	0.05	0.23
f_4	86.30	85.35	ζ_4	0.02	0.22
f_5	148.59	147.15	ζ_5	0.04	0.07
f_6	203.75	196.05	ζ_6	0.08	0.20
f_7	312.50	301.46	ζ_7	0.03	0.18
f_8	314.01	308.63	ζ_8	0.02	0.09
f_9	439.29	429.52	ζ_9	0.01	0.03
f_{10}	465.11	464.32	ζ_{10}	0.02	0.09

modal damping ratios extracted by the modal analysis. Note that the damping ratios for the jointed frame are relatively low, with the highest being 0.26%; for the monolithic frame the damping ratios are less than 0.08% for all modes. This is a good indication that the welded corners of the frames and the lumped-mass joints are not exhibiting much microslip. We also note that the 10th mode corresponds to little motion of the longitudinal beam of the frame where the joint is located, with most of the motion localized to the short beams (cf. Fig. 15). That the joint does not experience much motion in this mode explains the observation that its natural frequency does not vary much when the joint is added.

The technique described in the previous section was employed to study the non-linear damping effects in the dynamics due to the joint. It was decided not to examine the damping characteristics of all of the modes for the jointed frame. The analysis of Structure I established a pattern for the non-linear damping due to the joint, and it was desired only to see if the same pattern would be observed for the jointed Structure II. For both jointed and monolithic frames, studying the modal damping ratios for the closely spaced pairs of modes was difficult; indeed, the transient signals showed a beat phenomenon, confirming that the modes were interacting with a closely spaced companion mode. This is the reason why for the ensuing analysis only the modes close to 60, 150 and 300 Hz were examined for the jointed beam. The transient responses from the sensing positions were filtered by a 10th order Butterworth filter to focus at the free decay of one mode at a time. Because the modes considered were well separated from the other modes of the structure, the modal envelopes and modal damping ratios were calculated as described in Section 2.

In general, the results of the time-domain experiments followed the same trends as were observed for Structure I. The data were more difficult to post-process, however. Apart from the previously mentioned closely spaced pairs of modes leading to beat phenomena, another problem was that the modes of the frames were more densely spaced, compared to the modes of the beams studied in the previous section. Structure I possessed 5 modes under 2000 Hz, making them widely spaced and easy to filter; the frame, however, had 10 modes under 500 Hz, which were more difficult to filter effectively.

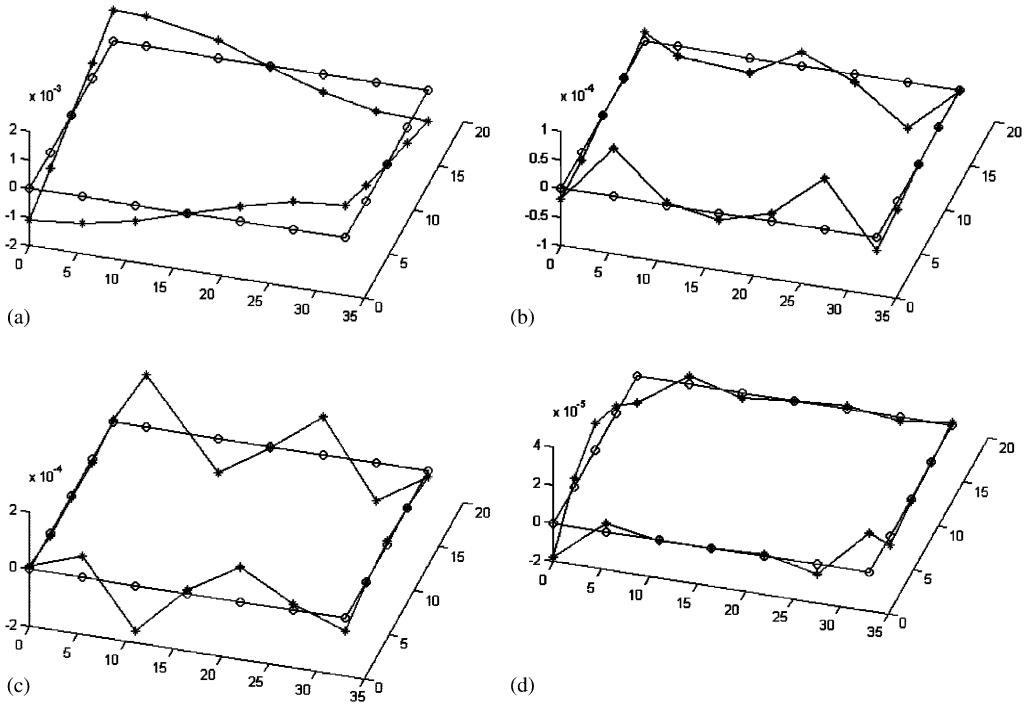

Fig. 15. Experimentally determined mode shapes of the monolithic frame: (a) mode 1, (b) mode 7, (c) mode 8 and (d) mode 11.

The time response for mode 3 of the monolithic frame, along with the logarithm of the envelope, is shown in Fig. 16. Note the relatively low level of damping of this mode, which can be attributed to the fact that for the monolithic structure only material damping is present (the welded joints in the corners and at the lumped mass do not contribute to damping due to the absence of microslip in these locations). Also note that the logarithm of the envelope in Fig. 16 is a straight line, indicating linear viscous damping. This time response is typical of the modes of the monolithic structure. Figs. 17–19 depict the filtered time responses and envelope logarithms for the 3rd (at 60 Hz), 5th (at 147 Hz), and 7th modes (at 301 Hz) of the jointed frame. These plots show similar characteristics as those seen for the jointed beam. The initial decay of the envelopes is quite rapid, with the logarithm of the envelopes following a curve indicating non-linear joint effects. Once the level of vibration subsides the envelopes approach exponential decay limits. The 5th mode shows slower decay and a nearly straight envelope logarithm; it was found that this mode has a node at the joint, resulting in less motion and curvature over the joint during vibration in this mode and, hence, minimal joint effects on the response. Figs. 20–22 depict the modal damping ratios plotted against magnitude of vibration for the 3rd, 5th, and 7th modes of the jointed frame. These curves were established by dividing the envelope into 50 intervals and calculating an average slope and magnitude of vibration for each interval. These curves also show similar trends as seen for the jointed beam. The 3rd and 7th modes correspond to relatively large motions at the joint, and as a result the modal damping ratios start fairly high (around 1%); the

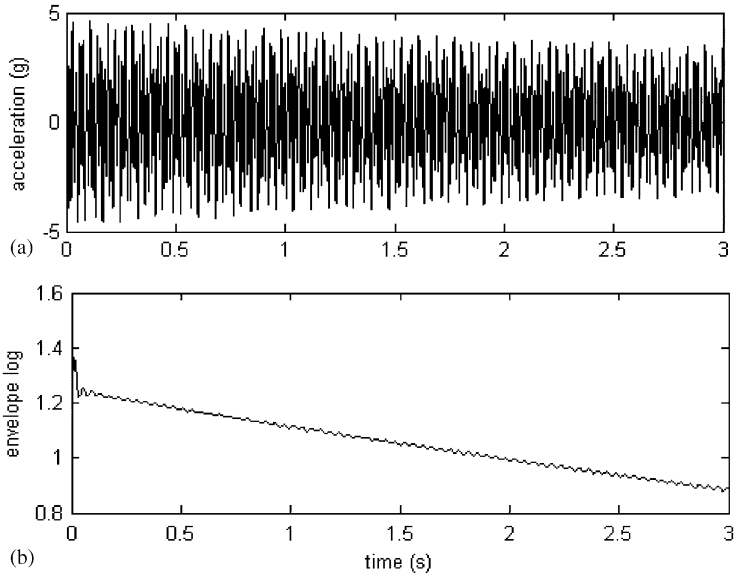

Fig. 16. (a) Filtered transient response and (b) logarithm of the envelope for the third mode (62 Hz) of the monolithic frame.

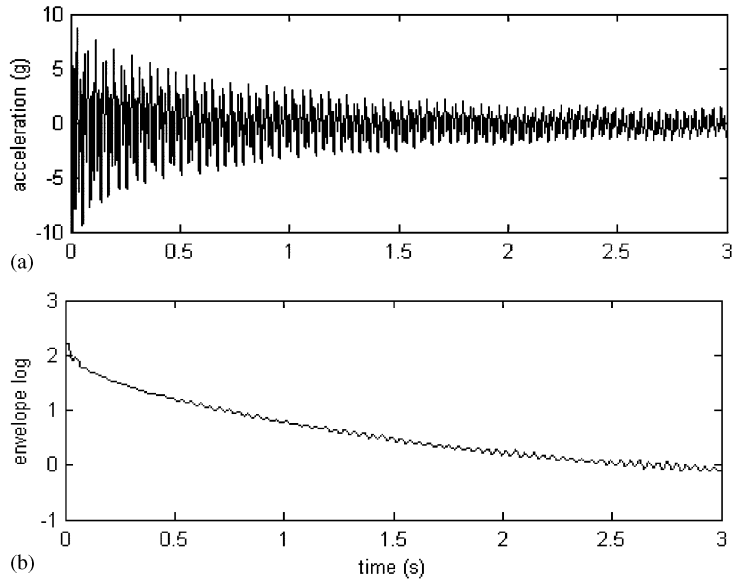

Fig. 17. (a) Filtered transient response and (b) logarithm of the envelope for the third mode (60 Hz) of the jointed frame.

vibration quickly subsides, however, and the damping decreases to much smaller values. As mentioned previously, for the 5th mode the non-linear effects are nearly negligible because that mode displays a node close to the joint.

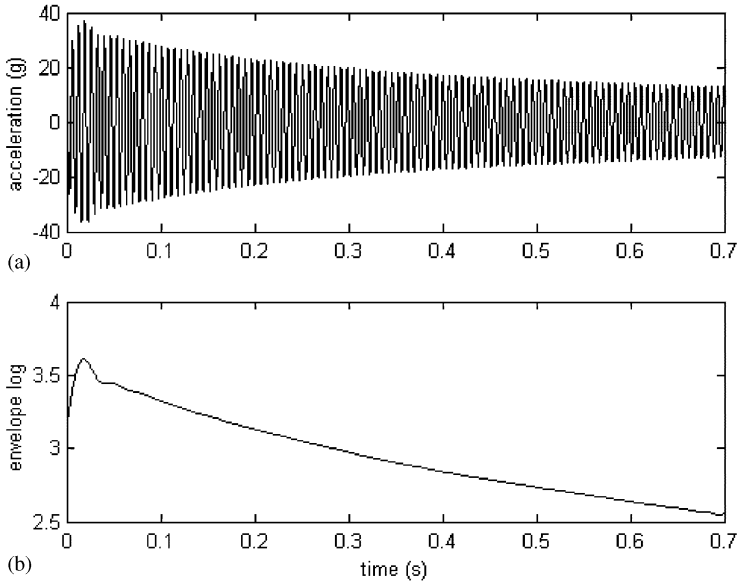

Fig. 18. (a) Filtered transient response and (b) logarithm of the envelope for the fifth mode (147 Hz) of the jointed frame.

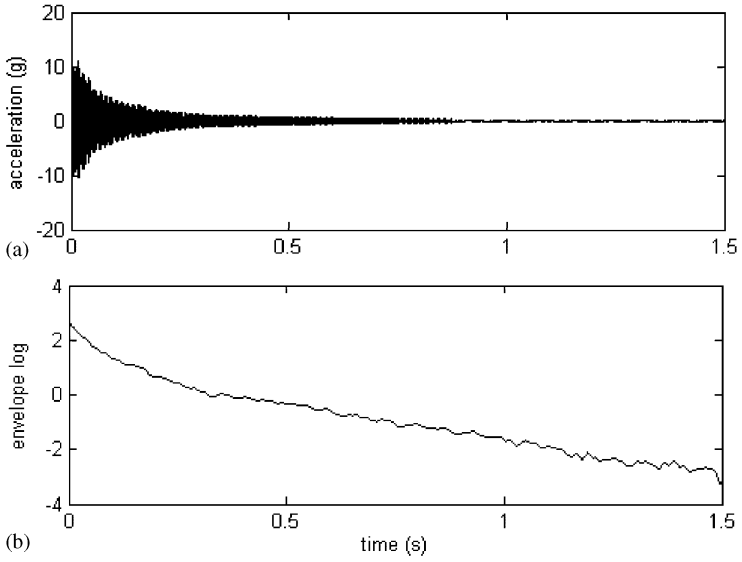

Fig. 19. (a) Filtered transient response and (b) logarithm of the envelope for the seventh mode (301 Hz) of the jointed frame.

In the next section we discuss the suitability of the Iwan model (a mathematical model for the shear lap joint) for capturing the joint effects. We show that using this model the non-linear joint damping effects observed in the experiments can be captured.

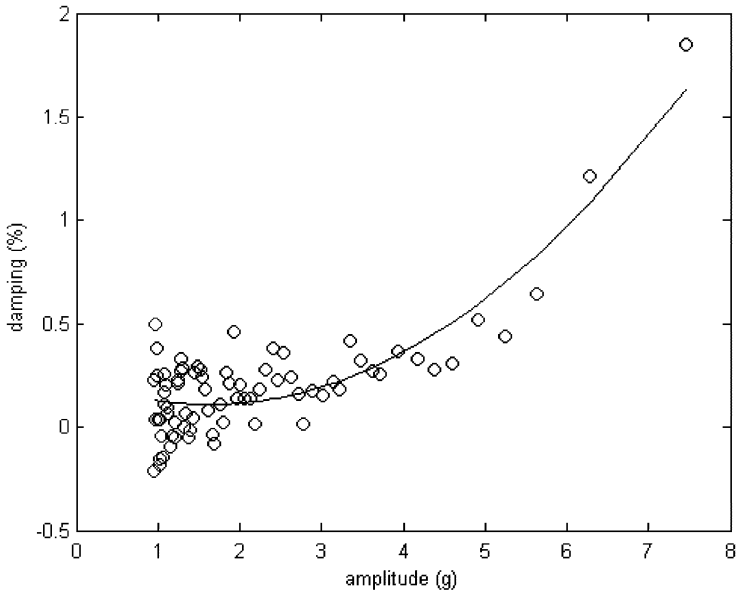

Fig. 20. Equivalent viscous damping ratio vs. vibration magnitude for the third mode of the jointed frame (60 Hz): symbols, experimental data; solid curve, fitted function.

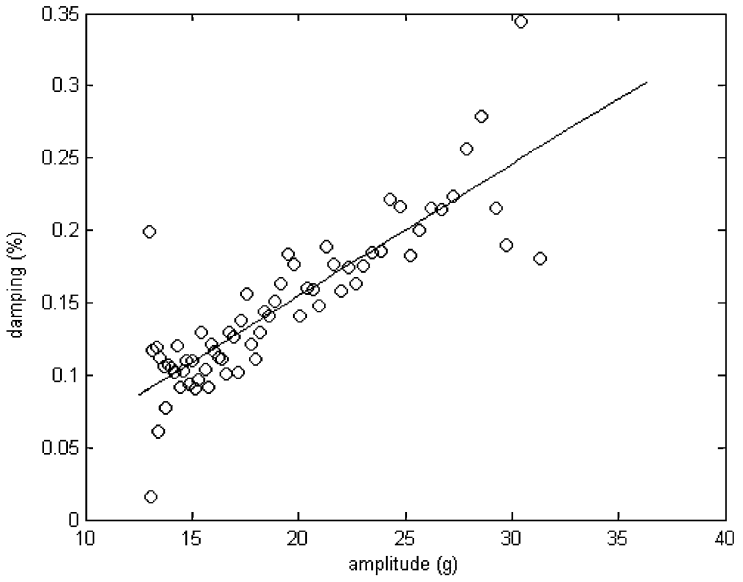

Fig. 21. Equivalent viscous damping ratio vs. vibration magnitude for the fifth mode of the jointed frame (147 Hz): symbols, experimental data; solid curve, fitted function.

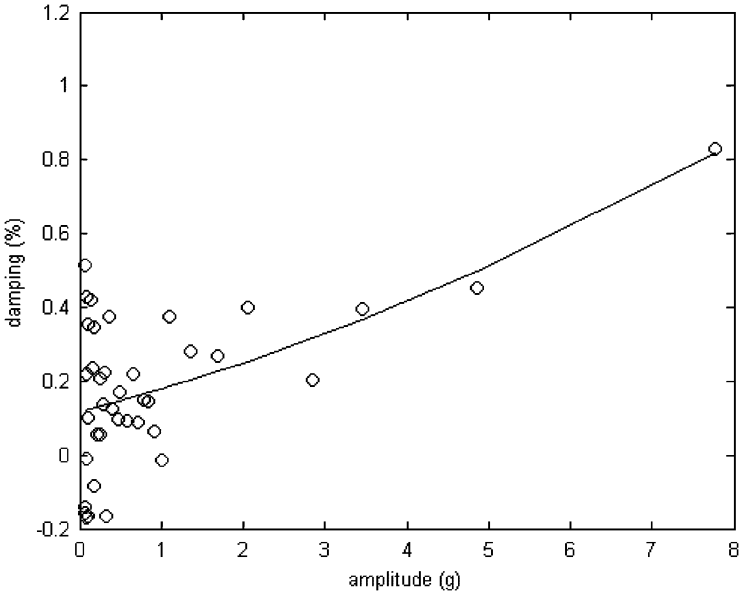

Fig. 22. Equivalent viscous damping ratio vs. vibration magnitude for the seventh mode of the jointed frame (301 Hz): symbols, experimental data; solid curve, fitted function.

4. Suitability of Iwan models for capturing the joint effects

Thus far, this work has been concerned with determining the significant effects a bolted lap joint imposes on structures of simple geometry undergoing bending motion:

- Generally, the natural frequencies diminish in the jointed structures; i.e., the structures exhibit softening stiffness behaviors.
- The damping is higher and amplitude-dependent in the jointed structures; i.e., they exhibit hardening damping behavior.
- Although not discussed in this work, the mode shapes of the jointed structures distort slightly compared to those of the monolithic structures [15].
- Energy is dissipated in a power-law relation with respect to the applied force.

Although this represents an incomplete list of the joint effects on the dynamics, an accurate mathematical model of the joint should take into account at least these effects.

As mentioned previously, the ultimate aim of the authors is to develop a reduced-order model that is capable of replicating the experimentally observed joint effects in a FE analysis. Although it is not necessarily the authors' intent to model the microphysics of the joint, it is desired to adopt a physics-based model to describe the dynamics at the joint itself. This means that the governing physics of the model should phenomenologically agree (at least in a simplified fashion) with what is thought to occur within a vibrating shear lap joint. In addition, the joint model will need to

incorporate a mechanism for reducing the stiffness and increasing the energy dissipation in a power-law relationship as more force is applied.

A model that intuitively seems capable of modelling the shear lap joint is the *Iwan model* [11], which was originally developed to model plasticity in structures. The model consists of a network of springs and frictional sliders, with each spring placed in series with a slider referred to as a Jenkins element [17]. An infinite number of these combined elements is then placed in parallel, resulting in the Iwan model. The *adjusted Iwan model* [18–20] is obtained by adding a single spring in parallel with the collection of Jenkins elements so that the joint exhibits some stiffness even during macroslip, as has been observed experimentally [4]. This one-dimensional adjusted Iwan model can be extended to the framework of FE analysis, resulting in the two-dimensional [18,19] and three-dimensional [20] *adjusted Iwan beam elements* (AIBEs).

The question must now be asked if the Iwan model is capable of reproducing the joint effects. As discussed above, the model intuitively seems to be appropriate, since it is capable of describing varying amounts of slip as a function of force, from microslip through to macroslip, and it allows for amplitude-dependent stiffness and damping. However, it remains to be shown if the model can reproduce the important joint effects found in our experimental analysis. Hence, the AIBE was used to model locally the shear lap joint in a FE model of the jointed Structure I under half-sine transient loading. The half-sine pulse had a duration of 0.001 s and an amplitude of 20, 50 or 100 lbf. The transient structural acceleration responses were computed, and from these, inertance FRFs and modal free-decay envelopes were found in order to determine if the AIBE captured the desired effects. These results were compared to those computed from a monolithic FE model of Structure I, composed of regular linear elastic beam elements.

The basic FE model was constructed using three-dimensional Euler–Bernoulli beam elements. The mesh incorporated only 9 elements to model the beam, which represents a relatively coarse mesh. Just 1 element was used to represent the center of the beam, where the joint is located. In the jointed model, the single element modelling the center of the beam was replaced with an AIBE. The stiffness and slip stress parameters of the Iwan elements were chosen arbitrarily; however, the slip-stress distribution function was band-limited. This type of distribution function leads to relatively simple modelling mathematics. For more details of the AIBE we refer to Refs. [18–20].

In Fig. 23 we depict a comparison of the driving-point inertance FRFs of the two FE models at location 4. Since the model parameters were chosen arbitrarily, only a qualitative analysis is possible; however, the plots show the correct trends. The natural frequencies have all shifted down in the jointed model, in agreement with what was observed experimentally. Moreover, for the jointed model the peaks are shorter and wider, which indicates higher damping. The 3rd peak ($\sim$760 Hz) does not show up very strongly on the jointed FRF, while it does in the monolithic case; this is in full agreement with experimental observations and was attributed to mode shape distortion of the jointed beam. Indeed, for the monolithic beam this mode has a node very near the point of measurement for the FRFs, meaning that it is difficult to measure it with this driving-point FRF; the distortion of this mode shape in the jointed beam places the node at the measurement location, thus completely eliminating the 3rd mode from the driving point inertance. Hence, the AIBE seems to cause mode shape distortions similar to those observed experimentally.

The transient modal responses of the beams with and without the AIBE were measured by filtering the transient responses with a 10th order Butterworth filter. Here we present results only for the 1st beam mode. Fig. 24 shows the modal response and its corresponding envelope decay

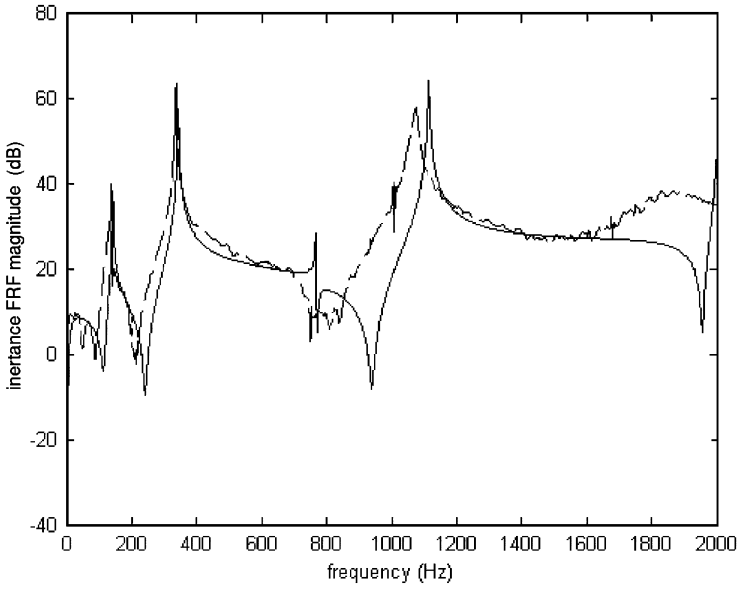

Fig. 23. Comparison of driving point inertance FRFs for the FE models with (light, broken curve) and without (dark, solid curve) the AIBE.

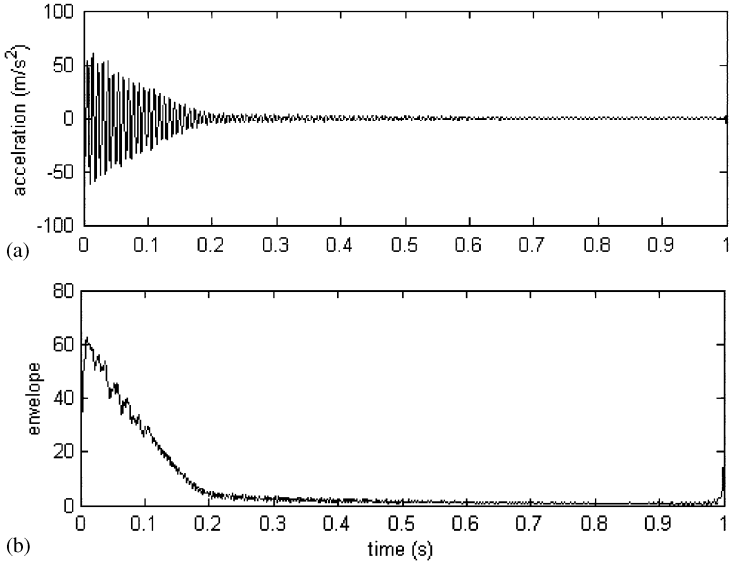

Fig. 24. (a) Filtered transient response and (b) envelope decay for the first mode of the beam with AIBE.

following the application of a high-magnitude impulsive force. Similar to experimental observations, the initial transient response (when the amplitude is high) shows a high decay rate which is nearly linear. This is because of the Coulomb-type sliding friction present at the

slider interfaces which produces a linearly decaying oscillation. Once the magnitude of the vibration subsides to the point where all the sliders stick, the response follows a gradual exponential decay. Qualitatively, this is the experimentally observed trend—strong damping at high amplitudes of vibration, low damping at low amplitudes. However, the linear decay during the initial phase of the motion was not observed in the experimental data, or at least it was much less pronounced. A different distribution function than the limited band one considered here might show a smoother transition from the high- to low-amplitude decay. For example, if the distribution was a smooth function that allowed a small number of sliders to move at low force and increasingly more with higher force, the envelope decay might agree better with the experimentally observed one.

Summarizing, the AIBE seems capable of capturing the amplitude-dependent stiffness and damping present in the jointed structure, since it reproduces the anticipated qualitative changes in the modal parameters when the joint is added. The overall stronger non-linear character of the Iwan model produces noise in the simulations which is not seen in the experimental results. However, this strong non-linear character might be controlled with different slip-stress distribution functions. Hence, we reach the conclusion that, with appropriate revisions, the Iwan model is a promising candidate for accurately reproducing the effects in the structural dynamics contributed by a shear lap joint.

5. Concluding remarks

Rather than try to investigate the microphysics present in a shear lap joint, a methodology was devised to experimentally investigate the effects of the joint on two structures composed of beam elements. Structure I was a simple beam with the joint located at its center, while Structure II was a rectangular frame with the joint in the center of one of its longitudinal beams. A basic feature of the methodology adopted was to test the jointed structures alongside their monolithic counterparts in an effort to discern the important effects the joint had on the dynamics. Tests included modal analysis, time-domain analysis, and energy dissipation analysis. FE analyses of the beam structure were carried out in order to reproduce the experimental results (see also the companion works [15,19]).

The various tests performed on the two structures showed several effects on the dynamics attributed to the shear lap joint: shifting down of the natural frequencies due to softening stiffness; non-linear hardening damping effects; and slight distortions of the mode shapes, which can alter drastically the measured FRFs through relocation of nodes. An energy dissipation analysis was conducted on the structures to gain further insight into the non-linear damping effects introduced by the joint. It was found that energy was dissipated in a power-law relationship to the input force, as expected from theoretical arguments. The monolithic Structure I showed a power-law exponent slightly higher than 2, with unmodelled effects in the shaker and the boundary conditions likely contributing to the higher value. The corresponding exponent for the jointed beam was closer to 3, again in agreement with theoretical expectations.

The Iwan model was examined as a possible way of capturing the experimentally observed joint effects. The model is composed of a network of springs and sliders and is capable of describing the range of joint motion from microslip to macroslip. A two-dimensional extension of this model,

the adjusted Iwan beam element (AIBE), was included in a FE model of Structure I in order to test its efficacy to model shear lap joint effects. It was found that the AIBE is capable of capturing the main stiffness and damping joint effects. Other studies have shown that the Iwan model is capable of describing the power-law relation between energy dissipated per cycle and input force with various exponents [12,13]. We conclude that AIBE holds promise for accurately modeling joint effects in the dynamics of practical structures.

Acknowledgements

This work was supported in part by the Department of Energy through Sandia National Laboratories and by the Office of Naval Research. The authors would like to thank Dr. Daniel Segalman of Sandia National Laboratories for sharing his many insights into this problem.

References

[1] M. Groper, Microslip and macroslip in bolted joints, *Experimental Mechanics* 25 (1985) 171–174.
[2] C.F. Beards, Damping in structural joints, *Shock and Vibration Digest* 23 (1991) 3–5.
[3] C.F. Beards, The damping of structural vibration by controlled interfacial slip in joints, *Journal of Vibration, Acoustics, Stress, and Reliability in Design* 105 (1983) 369–372.
[4] L. Gaul, J. Lenz, Nonlinear dynamics of structures assembled by bolted joints, *Acta Mechanica* 125 (1997) 169–181.
[5] L.E. Goodman, A review of progress in analysis of interfacial slip damping, in: *Structural Damping, Proceedings of the American Society of Mechanical Engineers Annual Meeting*, Atlantic City, 1959, pp. 35–48.
[6] R.D. Mindlin, Compliance of elastic bodies in contact, *Journal of Applied Mechanics* 16 (1949) 259–268.
[7] D.L. Gregory, D.O. Smallwood, R.G. Coleman, M.A. Nusser, Experimental studies to investigate damping in frictional shear joints, in: *Proceedings of 70th Shock and Vibration Symposium*, 1999.
[8] D.O. Smallwood, D.L. Gregory, R.G. Coleman, Damping investigations of a simplified frictional shear joint, in: *Proceedings of 71st Shock and Vibration Symposium*, 2000.
[9] D.O. Smallwood, D.L. Gregory, R.G. Coleman, A three parameter constitutive model for a joint which exhibits a power law relationship between energy loss and relative displacement, in: *Proceedings of the 72nd Shock and Vibration Symposium*, 2001.
[10] D.W. Lobitz, D.L. Gregory, D.O. Smallwood, Comparison of finite element predictions to measurements from the Sandia microslip experiment, in: *Proceedings of International Modal Analysis Conference*, Orlando, FL, 2001.
[11] W.D. Iwan, On a class of models for the yielding behavior of continuous and composite systems, *Journal of Applied Mechanics* 89 (1967) 612–617.
[12] D.J. Segalman, An initial overview of Iwan modeling for mechanical joints, Report SAND 2001-0811, Sandia National Laboratories, Albuquerque, NM, 2001.
[13] D.J. Segalman, personal communication, 2002.
[14] X. Ma, L.A. Bergman, A.F. Vakakis, System identification of bolted joints through laser vibrometry, *Journal of Sound and Vibration* 246 (3) (2001) 441–460.
[15] C.J. Hartwigsen, Dynamics of Jointed Beam Structures: Computational and Experimental Studies, M.Sc. Thesis, Department of Mechanical and Industrial Engineering, University of Illinois at Urbana-Champaign, 2002.
[16] H.R. Kess, N.J. Rosnow, B.C. Sidle, Effects of bearing surfaces on lap joint energy dissipation, Technical Report, Sandia National Laboratories, Albuquerque, NM, 2001.
[17] W.D. Iwan, A distributed-element model for hysteresis and its steady state dynamic response, *Journal of Applied Mechanics* 88 (Series E) (1966) 893–900.

[18] Y. Song, C.J. Hartwigsen, L.A. Bergman, A.F. Vakakis, A phenomenological model of a bolted joint, in: *Proceedings of the 2002 American Society of Civil Engineers, Engineering Mechanics Conference*, New York, paper 332, 2002.

[19] Y. Song, C.J. Hartwigsen, D.M. McFarland, A.F. Vakakis, L.A. Bergman, Simulation of dynamics of beam structures with bolted joints using adjusted Iwan beam elements, *Journal of Sound and Vibration* 273 (1 + 2) (2004) 249–276 .

[20] Y. Song, C.J. Hartwigsen, L.A. Bergman, A.F. Vakakis, Athree-dimensional nonlinear reduced-order predictive joint model, *Earthquake Engineering and Engineering Vibration* 2 (1) (2003) 59–73.